Běhounekite, U(SO₄)₂(H₂O)₄, from Jáchymov (St Joachimsthal), Czech Republic: the first natural U⁴⁺ sulphate

J. Plášil[1,2,*], K. Fejfarová[3], M. Novák[2], M. Dušek[3], R. Škoda[2], J. Hloušek[4], J. Čejka[5], J. Majzlan[6], J. Sejkora[5], V. Machovič[7,8] and D. Talla[2,9]

[1] Mineralogical Crystallography, Institute of Geological Sciences, University of Bern, Freiestrasse 3, CH-3012, Bern, Switzerland
[2] Department of Geological Sciences, Masaryk University, Kotlářská 2, Brno, 611 37, Czech Republic
[3] Institute of Physics ASCR, v.v.i., Na Slovance 2, Praha 8, 182 21, Czech Republic
[4] U Roháčových kasáren 24, Praha 10, 100 00, Czech Republic
[5] Department of Mineralogy and Petrology, National Museum, Václavské náměstí 68, Praha 1, 115 79, Czech Republic
[6] Institute of Geosciences, Friedrich-Schiller University, Burgweg 11, D-07749 Jena, Germany
[7] Institute of Chemical Technology, Prague, Technická 5, Praha 6, 166 28, Czech Republic
[8] Institute of Rock Structures and Mechanics, Academy of Science of Czech Republic, V Holešovičkách 41,182 09 Praha 8, Czech Republic
[9] Institute of Mineralogy and Crystallography, University of Vienna, Althanstrasse 14, A-1090 Wien, Austria

ABSTRACT

Běhounekite, orthorhombic $U(SO_4)_2(H_2O)_4$, is the first natural sulphate of U^{4+}. It was found in the Geschieber vein, Jáchymov (St Joachimsthal) ore district, Western Bohemia, Czech Republic, crystallized on the altered surface of arsenic and associated with kaatialaite, arsenolite, claudetite, unnamed phase UM1997-20-AsO:HU and gypsum. Běhounekite most commonly forms short-prismatic to tabular green crystals, rarely up to 0.5 mm long. The crystals have a strong vitreous lustre and a grey to greenish grey streak. They are brittle with an uneven fracture and have very good cleavage along {100}. The Mohs hardness is about 2. The mineral is not fluorescent either in short- or long-wavelength UV radiation. Běhounekite is moderately pleochroic, α~β is pale emerald green and γ is emerald green, and is optically biaxial (+) with α = 1.590(2), β = 1.618(4), γ = 1.659(2) (590 nm), 2V (calc.) = 81°, birefringence 0.069. The empirical formula of běhounekite (based on 12 O atoms, from an average of five point analyses) is $(U_{0.99}Y_{0.03})_{\Sigma1.02}(SO_4)_{1.97}(H_2O)_4$. The simplified formula is $U(SO_4)_2(H_2O)_4$, which requires UO_2 53.77, SO_3 31.88, H_2O 14.35, total 100.00 wt.%. Běhounekite is orthorhombic, space group *Pnma*, a = 14.6464(3), b = 11.0786(3), c = 5.6910(14) Å, V = 923.43(4) Å³, Z = 4, D_{calc} = 3.62 g cm⁻³. The seven strongest diffraction peaks in the X-ray powder diffraction pattern are [d_{obs} in Å (I) (*hkl*)]: 7.330 (100) (200), 6.112 (54) (210), 5.538 (21) (020), 4.787 (42) (111), 3.663 (17) (400), 3.478 (20) (410), 3.080 (41) (321). The crystal structure of běhounekite has been solved by the charge-flipping method from single-crystal X-ray diffraction data and refined to R_1 = 2.10 % with a *GOF* = 1.51, based on 912 unique observed diffractions. The crystal structure consists of layers built up from [8]-coordinate uranium atoms and sulphate tetrahedra. The eight ligands include four oxygen atoms from the sulphate groups and four oxygen atoms from the H_2O molecules. Each uranium coordination polyhedron is connected via sulphate tetrahedra with other uranium polyhedra and through hydrogen bonds to the apices of sulphate tetrahedra. The dominant features of the Raman and infrared spectra of běhounekite are related to stretching vibrations of SO_4 tetrahedra (~1200–950 cm⁻¹), O–H stretching modes (~3400–3000 cm⁻¹) and H–O–H bending modes (~1650 cm⁻¹). The mineral is named in honour of František Běhounek, a well known Czech nuclear physicist.

Introduction

THE geochemical behaviour of uranium is controlled by the properties of its two common oxidation states, U^{4+} and U^{6+}. The former state is highly insoluble and typical of primary minerals, the latter is characteristic of alteration phases (Langmuir, 1978; Finch and Murakami, 1999). There is just one supergene mineral with U^{4+} in its crystal structures, ianthinite, $[U^{4+}(UO_2)_4O_6(OH)_4 (H_2O)_4](H_2O)_5]$ (Burns *et al.*, 1997). Here, we describe a secondary sulphate of U^{4+}, the new mineral běhounekite, for the first time.

Běhounekite is named in honour of Professor František Běhounek who was born on October 28, 1898 in Prague and died on January 1, 1973 in Karlovy Vary. He was a famous Czech nuclear physicist and studied under the supervision of Marie Curie-Sklodowska at the Sorbonne. Professor Běhounek founded the National Institute for Radiology (he later became the head of the Institute), the Institute of Atmospheric Electricity and the Institute for Radiotherapy. As well as scientific papers, he wrote non-fiction and science-fiction, totalling more than 65 publications.

The new mineral and its name have been approved by the Commission on New Minerals, Nomenclature and Classification of the International Mineralogical Association (IMA 2010-046) (Plášil *et al.*, 2011). The holotype specimen is deposited in the mineralogical collections of the National Museum in Prague, Czech Republic, catalogue number P1p 2/2010.

Occurrence

Běhounekite was found in the Geschieber vein (10th level, Svornost/Einigkeit shaft) at the intersection with the Geier vein structure at Jáchymov, Western Bohemia, Krušné hory mountains, Czech Republic (50º 22′ 21.138 N, 12º 54′ 46.251 E). Detailed information about the mineralogy, geology and mineral paragenesis of the deposit, as well as the mining history, is provided in Ondruš *et al.* (1997*a*, 2003) and in Tvrdý and Plášil (2010) and references therein. The samples examined in this study were collected in 1980s by one of us (JH).

Běhounekite is a very rare secondary mineral that was found on material collected from the footwall of the mine adit. Arsenic is the dominant primary mineral in the běhounekite-bearing assemblage and arsenopyrite, pyrite (locally As-rich), rare proustite and silver are also present. Běhounekite occurs on highly altered arsenic and in direct association with a phase related to trögerite, gypsum, arsenolite, kaatialaite, claudetite and an as yet uncharacterized mineral, UM1997-20-AsO:HU (Ondruš *et al.*, 1997*b*; Smith and Nickel, 2007).

Physical and optical properties

Běhounekite is most commonly found as short-prismatic to tabular crystals (Figs 1 and 2) and less commonly as long prismatic crystals (Figs 3 and 4); the two types may occur together. The more common short prismatic crystals are up to 0.5 mm long. The chemical composition and powder XRD data are identical for both.

Běhounekite is green, with a vitreous lustre, and is translucent to transparent. It has a grey to greenish grey streak. Its Mohs hardness is ~2. It is not fluorescent in either long- or short-wavelength UV radiation. It is brittle, with an uneven fracture and very good cleavage along {100}. The density was not measured directly, but was calculated on the basis of the unit-cell parameters and chemistry: $D_{calc} = 3.62$ g cm^{-3}. Běhounekite is moderately pleochroic, $\alpha \sim \beta$ is pale emerald green and γ is emerald green. Both crystal types have similar optical properties, but the refractive
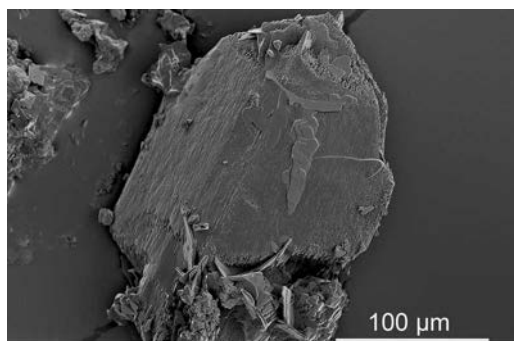

FIG. 1. An SEM image of a euhedral crystal of běhounekite with an obviously corroded surface, partly overgrown by the later tabular crystal aggregates of the same phase.

Fig. 2. Euhedral green and prismatic light green (see Fig. 4) crystals of běhounekite on altered arsenic with arsenolite (partly in matrix) and an additional long prismatic (needle-like) phase which is a non approved new mineral. Field of view 4 mm; photo P. Škácha.

indices were measured only on the short prismatic crystals. The refractive indices α and γ were measured in the plane of good cleavage (100); β is perpendicular to the elongation of both short prismatic and long prismatic crystals. Běhounekite is optically biaxial (+) with α = 1.590(2), β = 1.618(4), γ = 1.659(2) (590 nm), 2V (calc.) = 81º, birefringence 0.069.

Chemical composition

The chemical composition of běhounekite was determined using a Cameca SX100 electron microprobe operating in wavelength-dispersive mode at an accelerating voltage of 15 kV, current

Fig. 3. Long thick prismatic crystals of běhounekite on altered arsenic. Field of view 4 mm; photo J. Hloušek.

of 5 nA and beam diameter of 10 μm. These conditions were used to minimize damage due to the electron beam during major-element analysis. The rare earth elements were analysed afterward at an accelerating voltage of 15 kV, beam current of 60 nA and beam diameter of 10 μm. The following X-ray lines and standards were selected to minimize line overlaps: $K\alpha$ lines: S (baryte); $L\alpha$ lines: Y (YAG), Ce (CePO$_4$), Sm (SmF$_3$), Gd (GdF$_3$), Dy (DyPO$_4$), Er (YErAG), Yb (YbPO$_4$); $L\beta$ lines: Nd (NdPO$_4$); $M\beta$ lines: U (U metal). The elements La, Pr, Eu, As, Sc, Al, Si, P, Na, Pb, Ca, Fe, V and Zr were also sought, but concentrations were below detection limits (0.02−0.10 wt.%). Peak counting times were 10−20 s for major elements and 40−60 s for minor or trace elements; the counting time on the background points was half of the peak counting time. Measured intensities were converted to elemental concentrations using the *PAP* (Pouchou and Pichoir, 1985) correction routine. Relative errors of measurement of U and S, calculated on the basis of one standard deviation, are approximately 6−8 rel.%.

The empirical formula of běhounekite (based on 12 O atoms and an average of 5 point analyses) is $(U_{0.99}Y_{0.03})_{\Sigma1.02}(SO_4)_{1.97}(H_2O)_4$ (Table 1). The simplified formula is $U(SO_4)_2(H_2O)_4$, which requires UO$_2$ 53.77, SO$_3$ 31.88, H$_2$O 14.35, total 100.00 wt.%. There is a small excess of positive charge (+0.11 charge units) in the empirical formula of běhounekite. The main cause of the
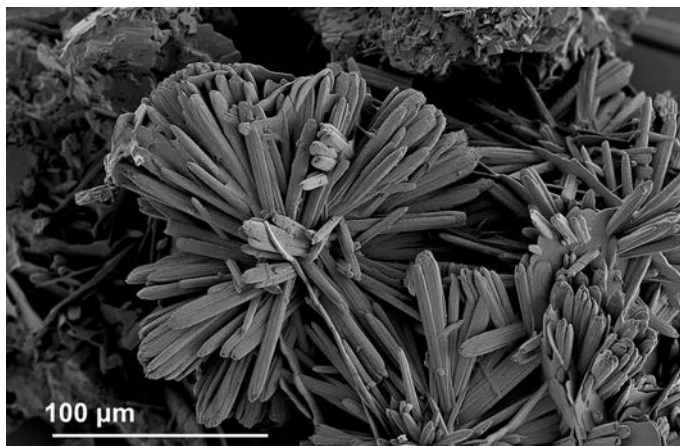
FIG. 4. An SEM image of prismatic thin crystals of běhounekite.

TABLE 1. The major and minor element composition of běhounekite from Jáchymov.

	1	2	3	4	5	Mean	St. dev.	D.L.	Theoretical composition
Y_2O_3	0.58	0.83	0.87	0.91	0.55	0.75	0.21	0.15	
SO_3	31.82	30.96	31.21	31.66	31.15	31.36	2.33	0.14	31.88
UO_2	53.80	52.87	52.69	53.88	53.78	53.40	3.09	0.81	53.77
H_2O*	14.60	14.47	14.45	14.78	14.55	14.53			14.35
Total	100.80	99.13	99.22	101.22	100.03	100.04			100.00
Y	0.026	0.038	0.040	0.040	0.025	0.033			
U^{4+}	0.993	0.996	0.988	0.993	1.007	0.994			1.000
S	1.981	1.967	1.973	1.967	1.968	1.969			2.000
H_2O	4.000	4.000	4.000	4.000	4.000	4.000			4.000
$OH^{\#}$	0.090	0.160	0.120	0.160	0.170	0.107			

	Mean	St. dev.	D.L.
La_2O_3	n.d.	0.07	0.1
Ce_2O_3	0.11	0.06	0.09
Pr_2O_3	n.d.	0.13	0.16
Nd_2O_3	0.26	0.11	0.15
Eu_2O_3	n.d.	0.15	0.19
Gd_2O_3	0.26	0.09	0.1
Dy_2O_3	0.2	0.1	0.12
Er_2O_3	0.06	0.05	0.06
Yb_2O_3	n.d.	0.07	0.08

Mean: mean of 1−5 (in wt.% oxide);
St. dev.: standard deviation (in wt.% oxide);
D.L.: detection limit (in wt.% oxide);
n.d.: below detection limit;
1−5: point analyses, a.p.f.u. coefficients calculated on the basis of Y + U + S = 3 atoms;
* H_2O content in wt.% calculated on the basis of a theoretical content of 4 H_2O in the crystal structure of běhounekite with the OH^- content derived from charge balance;
# OH calculated to maintain charge balance.

charge excess is likely to be the analytical difficulties that are typical of electron microprobe analyses of hydrated materials as a result of the decomposition of the sample under the electron beam.

Other *REE*s were detected in addition to Y, but běhounekite contains <0.02 a.p.f.u. of these in total. The mechanism by which Y^{3+} and *REE*$^{3+}$ are incorporated into the structure is not clear. Hydrogen can be excluded as a charge-balancing cation because no OH groups have been detected by vibrational spectroscopy (see below). The partial replacement of U^{4+} by U^{5+} as follows: $2U^{4+} \leftrightarrow U^{5+} + REE^{3+}$ is a possibility. The chondrite-normalized *REE*, Y plot (Fig. 5) exhibits enrichment in *MREE* (Sm and Gd) and depletion in *LREE* and *HREE*. The chondrite-normalized value of Y is slightly lower than that of Dy.

Thermal analysis of synthetic U(SO₄)₂(H₂O)₄

Thermal analysis of synthetic U(SO$_4$)$_2$(H$_2$O)$_4$

Thermogravimetric (TG) analysis of běhounekite could not be undertaken because of the lack of material. According to Chernyaev (1964), synthetic orthorhombic U(SO$_4$)$_2$(H$_2$O)$_4$ dehydrates in three partly overlapping steps: $1.5-2$ H$_2$O ($135-145$ºC), $2-3.5$ H$_2$O ($145-205$ºC) ($\Sigma 3.5$ H$_2$O) and 0.5 H$_2$O ($240-250$ºC). The oxidation of U^{4+} begins in the temperature interval $375-400$ºC. This oxidation process is connected with the formation of anhydrous UO$_2$SO$_4$ (~560ºC) and the release of SO$_2$. The UO$_2$SO$_4$ decomposes at $680-700$ºC with SO$_3$

FIG. 5. Chondrite-normalized pattern (after Taylor and McLennan 1985) of the *REE* and Y contents in běhounekite (based on analyses by wavelength-dispersive spectrometry).

release and UO$_{2.67}$ formation ($730-870$ºC). Simultaneous differential thermal analysis (DTA) shows that the dehydration and decomposition reactions are endothermic. Thermal analysis of synthetic U^{4+}(SO$_4$)$_2$(H$_2$O)$_4$ in a nitrogen atmosphere was studied by Leroy (1966, 1967) and Delobel (1970).

Vibrational spectroscopy

The Raman spectrum of běhounekite in the range $200-1900$ cm^{-1} (with a spectral resolution of 2 cm^{-1}) was collected using a LabramHR dispersive Raman spectrometer (Jobin Yvon) mounted on a confocal Olympus microscope. The Raman signal was excited by a 785 nm laser and detected by a multichannel air-cooled CCD camera. The Raman spectrum in the range $490-4000$ cm^{-1} was collected on a Renishaw RM1000 confocal micro-Raman spectrometer (resolution 2 cm^{-1}) using an excitation wavelength of 480 nm.

The Fourier-transform infrared spectrum (FTIR) of běhounekite was collected using a Nicolet 6700 FTIR spectrometer coupled to a Continuum microscope. A diffuse reflectance (DRIFTS) method was used and the spectrum was collected from $4000-650$ cm^{-1} with a resolution of 5 cm^{-1}. For manipulation and processing of the spectra, *Omnic Spectral Tools* software was used.

The vibrational spectra of synthetic and natural uranyl (i.e. U^{6+}) sulphates were reviewed by Čejka (1999, 2007). Information about the infrared and Raman spectra of U^{4+} sulphates is very limited (Umreiko and Nikanovich, 1984). Infrared spectra of synthetic U(SO$_4$)$_2$(H$_2$O)$_4$ were previously published by Leroy (1966, 1967). Factor group analysis for vibrational spectra of this synthetic compound together with an interpretation of its infrared spectrum was presented by Delobel (1970). Theoretical and experimental studies of the vibrational spectrum of synthetic U(SO$_4$)$_2$(H$_2$O)$_4$ were undertaken by Malinka *et al.* (1979, 1981). We note here that there are differences in the frequencies observed in vibrational spectra for synthetic compounds and natural minerals, related to the fact that natural minerals and synthetic 'analogues' may not be isostructural (Čejka and Urbanec, 1990; Hawthorne and Schindler, 2008; Schindler and Hawthorne, 2008).

The Raman and infrared spectra of běhounekite are shown in Figs 6−8. A band at 3387 cm^{-1} with shoulders at 3243 and 3088 cm^{-1} and Raman
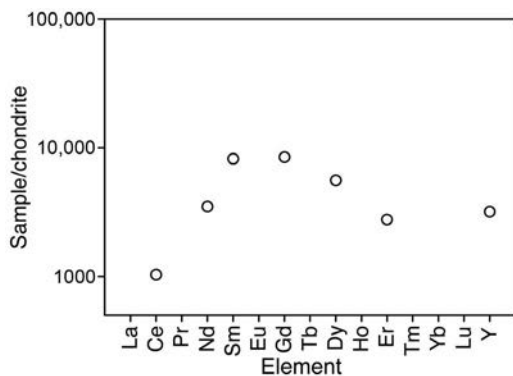
bands at 3370 and 3206 cm^{-1} are assigned to the ν O−H stretching vibrations of hydrogen bonded H$_2$O molecules. The O−H⋯O hydrogen bond lengths are ∼2.7−2.8 Å, according to the correlation provided by Libowitzky (1999). The O−H⋯O bond lengths obtained from our refined crystal structure are between 2.68 and 3.42 Å (mean 2.73 Å). Neither Raman nor infrared spectroscopy suggest the presence of OH groups in the structure of běhounekite. Infrared bands at 1674, 1645 and 1610 cm^{-1} are attributed to the ν$_2$ (δ) bending vibrations of structurally none-quivalent H$_2$O molecules. Leroy (1966, 1967) observed this band at 1635 cm^{-1}; Delobel (1970) described a broad band with a maximum at 3200 cm^{-1} and two bands at 1635 and 1630 cm^{-1}; Malinka et al. (1981) assigned three bands at 3350, 3230 and 2300 cm^{-1} to symmetrically distinct and strongly hydrogen bonded H$_2$O molecules. According to Delobel (1970), the structure contains two symmetrically distinct H$_2$O molecules whose point symmetries are C_i and C_s. Raman bands at 994 and 1023 cm^{-1} and an infrared band at 1019 cm^{-1} are assigned to the ν$_1$ (SO$_4$)$^{2-}$ symmetric stretching vibrations. Delobel (1970) attributed a weak infrared band at

1000 cm^{-1} and Malinka et al. (1979, 1981) two infrared bands at 960 and 1013 cm^{-1} in the case of the synthetic analogue to this vibration. Raman bands at 1269, 1251, 1177, 1158, 1102 and 1037 cm^{-1} (Fig. 7) are assigned to the split triply degenerate ν$_3$ (SO$_4$)$^{2-}$ antisymmetric stretching vibrations. Delobel (1970) observed two infrared bands at 1030 and 1000 cm^{-1}, Malinka et al. (1979, 1981) three infrared bands at 1218, 1150, 1100 cm^{-1}. Two of the Raman bands at 451, 438 and 417 cm^{-1} are connected with the split doubly degenerate ν$_2$ (SO$_4$)$^{2-}$ bending vibration. In the synthetic analogue of běhounekite, these infrared bands are located at 430 and 384 cm^{-1} (Malinka et al. 1979). The split triply degenerate ν$_4$ (SO$_4$)$^{2-}$ bending vibration is represented by Raman bands at 638, 619 and 598 cm^{-1}. Delobel (1970) observed corresponding infrared bands at 617 and 598 cm^{-1}, and Malinka et al. (1979, 1981) at 650, 632, 615 and 594 cm^{-1}. The observed bands are comparable with those calculated by Malinka et al. (1979, 1981) for the [U$_2$SO$_4$]$^{6+}$ fragment, point symmetry C_{2v} and the [U$_5$(SO$_4$)$_4$(H$_2$O)$_4$] fragment, point symmetry C_s. According to Malinka et al. (1979, 1981), the observed Raman bands at lower wavenumbers
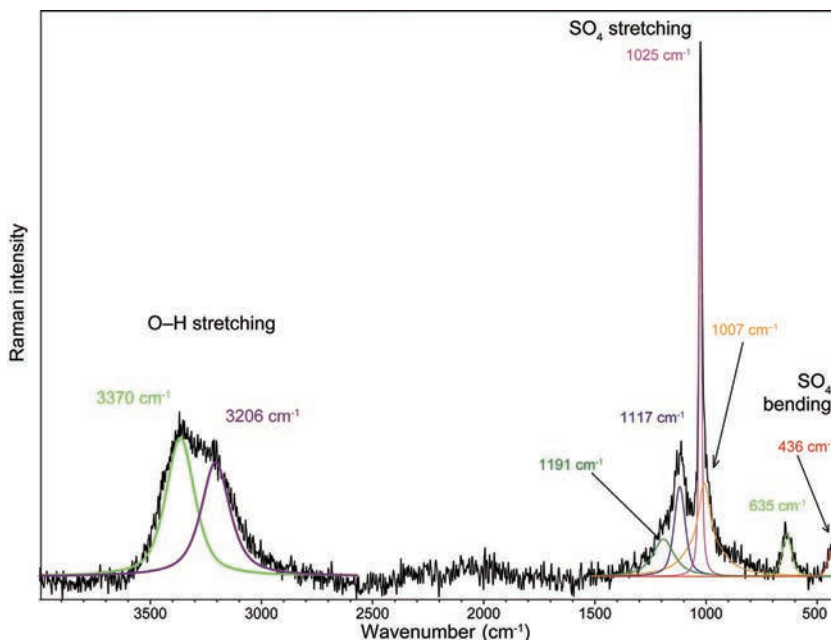
FIG. 6. The Raman spectrum of běhounekite in the range 4000−490 cm^{-1}. The bands corresponding to the O−H stretching modes are clearly visible at 3370 and 3206 cm^{-1}.
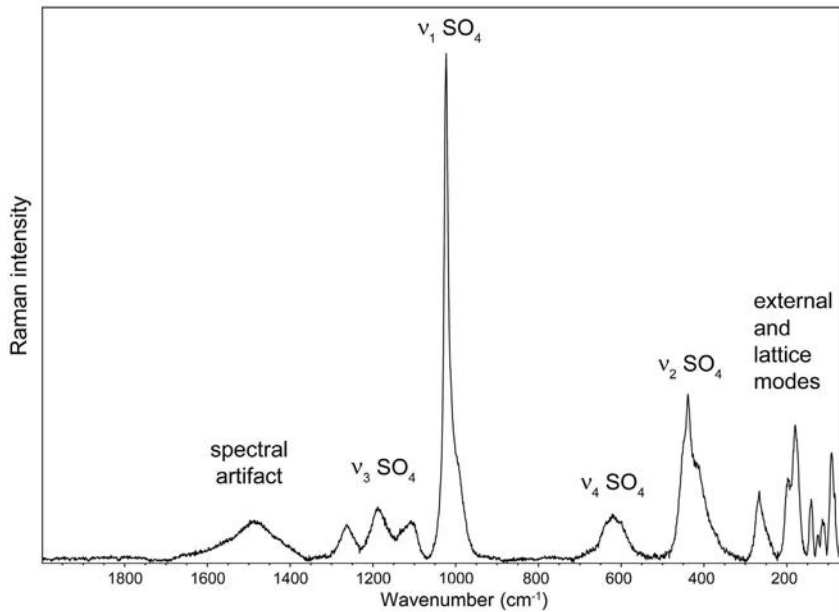
FIG. 7. The Raman spectrum of běhounekite in the range $1900-150$ cm^{-1}, with characteristic vibrational modes of SO$_4$ tetrahedra.
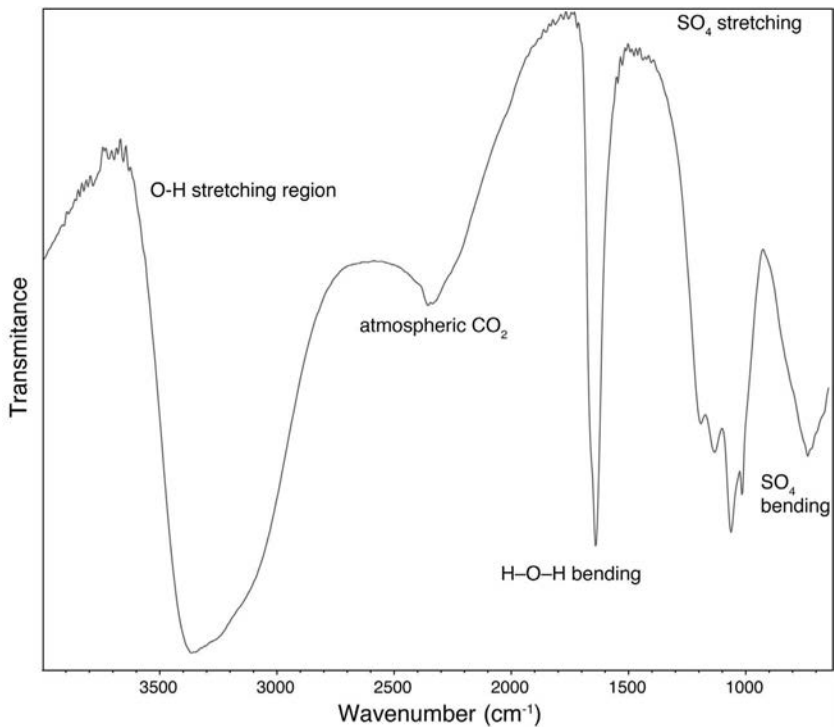

FIG. 8. The infrared spectrum of běhounekite showing characteristic vibrational features of H$_2$O molecules and SO$_4$ tetrahedra.

may be assigned as follows: 268 cm^{-1} to the ν U−SO$_4$ stretching vibration; 250 cm^{-1} to the ν U−H$_2$O stretching vibration; 198 and 178 cm^{-1} to the δ$_s$ H$_2$O−U−H$_2$O symmetric bending vibration; δ$_{as}$ H$_2$O−U−H$_2$O antisymmetric bending vibration; 125 and 116 cm^{-1} to (SO$_4$)$^{2-}$ rotation, and 92 cm^{-1} to the δ$_{as}$ H$_2$O−U−H$_2$O antisymmetric bending vibration.

X-ray crystallography and crystal structure determination

X-ray powder diffraction data for běhounekite were collected using a Bruker D8 Advance powder diffractometer, equipped with a LynxEye 1D solid-state detector, operating at 40 kV and 40 mA, using Ni-filtered Cu-*K*α radiation. A small amount of běhounekite was placed onto a zero-background (Si) holder, crushed in a drop of acetone, dried and scanned in Bragg-Brentano geometry. A 0.01º step size in the range 4º−70º2θ with variable counting time (total counting time was 23 h) was used, and the sample was rotated to improve the scattering statistics. For profile fitting of each diffraction maximum, *DIFFRAC*^{TM} *TOPAS* software version 4.2 (BrukerAXS) was employed. The pseudo-Voigt profile shape function corrected for

TABLE 2. Powder diffraction data for běhounekite from Jáchymov.

d_{obs}	d_{calc}	I_{obs}	h	k	l	d_{obs}	d_{calc}	I_{obs}	h	k	l
7.330	7.324	100	2	0	0	1.9670	1.9675	2	1	4	2
6.112	6.110	54	2	1	0	1.9327	1.9340	2	7	1	1
5.538	5.541	21	0	2	0	1.9159	1.9158	4	5	2	2
5.064	5.065	15	0	1	1	1.8965	1.8960	1	4	5	0
4.787	4.787	42	1	1	1	1.8555	1.8558	1	1	1	3
4.418	4.419	9	2	2	0	1.8467	1.8467	4	0	6	0
4.165	4.166	8	2	1	1	1.8321	1.8315	3	6	4	0
3.832	3.833	10	1	2	1	1.8064	1.8065	3	8	1	0
3.705	3.707	3	3	0	1	1.7873	1.7869	1	5	3	2
3.663	3.662	17	4	0	0	1.7437	1.7440	1	2	2	3
3.490	3.491	4	2	2	1	1.7388	1.7385	2	8	2	0
3.478	3.477	20	4	1	0	1.7346	1.7342	3	7	3	1
3.297	3.298	12	2	3	0	1.7215	1.7219	1	8	1	1
3.099	3.099	11	0	3	1	1.7085	1.7082	2	2	6	1
3.080	3.081	41	3	2	1	1.6879	1.6879	3	5	5	1
3.033	3.032	3	1	3	1	1.6864	1.6853	2	3	2	3
2.8536	2.8539	1	2	3	1	1.6674	1.6669	<1	7	1	2
2.7692	2.7702	6	0	4	0	1.6627	1.6627	<1	8	2	1
2.7101	2.7100	1	1	1	2	1.6462	1.6464	2	3	5	2
2.6914	2.6921	2	4	2	1	1.6135	1.6131	2	7	2	2
2.6007	2.6005	5	4	3	0	1.5840	1.5838	1	4	6	1
2.5378	2.5360	4	5	1	1	1.5767	1.5767	1	5	1	3
2.4946	2.4954	17	1	2	2	1.5643	1.5649	<1	9	0	1
2.4411	2.4414	5	6	0	0	1.5473	1.5472	<1	2	7	0
2.4005	2.4011	6	3	1	2	1.5396	1.5407	<1	1	6	2
2.3580	2.3584	4	2	4	1	1.5311	1.5312	<1	2	4	3
2.2350	2.2341	1	6	2	0	1.5274	1.5275	1	8	4	0
2.2310	2.2287	2	1	3	2	1.5063	1.5059	1	9	2	1
2.2188	2.2189	4	3	4	1	1.5031	1.5016	1	5	5	2
2.1990	2.1992	7	6	1	1	1.4721	1.4728	1	6	6	0
2.1282	2.1288	2	5	3	1	1.4516	1.4521	2	10	1	0
2.0655	2.0652	1	0	5	1	1.4399	1.4403	1	7	4	2
2.0597	2.0597	2	4	4	1	1.4021	1.4016	1	9	1	2
2.0460	2.0472	8	3	3	2	1.3860	1.3864	<1	2	1	4
2.0079	2.0080	3	5	1	2	1.3744	1.3742	<1	10	2	1
1.9883	1.9877	<1	2	5	1	1.3621	1.3625	2	9	4	1

TABLE 3. Unit-cell parameters of běhounekite from Jáchymov in comparison with the synthetic phase of Kierkegaard (1956).

	Kierkegaard (1956), powder	Jáchymov, powder	Jáchymov, single crystal
a (Å)	14.674(5)	14.650(2)	14.6464(3)
b (Å)	11.093(5)	11.082(2)	11.0786(3)
c (Å)	5.688(5)	5.695(3)	5.6910(14)
V (Å^3)	925.8	924.6(3)	923.43(4)

asymmetry (full-axial model) was used. The unit-cell parameters were refined from 72 reflections by a least-squares algorithm using *Celref* (LMGP Suite of Programs). The powder diffraction pattern of běhounekite (Table 2) is in good agreement with the calculated pattern and the pattern reported for synthetic material by Kierkegaard (1956). Refined unit-cell parameters of běhounekite from Jáchymov (Table 3) are similar to those of the synthetic phase.

TABLE 4. Crystallographic data and refinement parameters for běhounekite.

Crystal data

Structural formula	$U(SO_4)_2(H_2O)_4$
Crystal system	orthorhombic
Space group	*Pnma*
Unit-cell parameters a, b, c (Å)	14.6464(3), 11.0786(3), 5.6910(1)
	(based on 6,630 reflections)
Unit-cell volume (Å^3)	923.43(4)
Z	4
Calculated density (g cm^{-3})	3.613
Absorption coefficient (mm^{-1})	18.1
Crystal size (mm)	$0.23 \times 0.18 \times 0.12$
F_{000}	912

Data collection

Diffractometer	Oxford Diffraction GeminiA, Atlas CCD detector
Temperature (K)	297.2
Radiation, wavelength (Å)	Mo-Ka, 0.71073
θ range for data collection (º)	4.28−26.32º
h, k, l ranges	±7, ±13, ±18
Axis, frame width (º), time per frame (s)	ω, 0.75, 25
Total reflections collected	9,945
Unique reflections	990
Unique reflections $I > 3\sigma(I)$	912
Data completeness to θ_{max} (%)	99.65

Structure refinement by Jana2006

Refinement method	Full-matrix least-squares on F^2
No. of refined parameters, restraints	85, 7
Weighting details	$w = 1/(\sigma^2(I) + 0.0016I^2)$
R, wR [$I > 3\sigma(I)$]	0.0209, 0.0727
R, wR all data	0.0244, 0.0760
GOF	1.51
Largest diff. hole/peak (e Å^{-3})	−1.13/1.44

TABLE 5. Atomic positions and equivalent isotopic displacement parameters (Å^2) for the crystal structure of běhounekite.

Atom	x/a	y/b	z/c	U_{eq}
U1	0.82892(2)	0.75	0.12581(5)	0.0096(1)
S1	0.8508(1)	0.4451(1)	0.3856(2)	0.0094(4)
O1	0.9760(4)	0.75	0.308(1)	0.020(2)
O2	0.9244(3)	0.6247(5)	−0.1104(7)	0.021(1)
O3	0.8323(3)	0.5757(5)	0.3520(7)	0.019(2)
O4	0.9065(3)	0.4297(4)	0.5943(7)	0.017(1)
O5	0.7611(3)	0.3839(4)	0.4165(7)	0.018(1)
O6	0.8949(3)	0.3968(4)	0.1751(7)	0.019(1)
O7	0.7033(5)	0.75	0.3837(9)	0.021(2)
H1	0.701(4)	0.6896(14)	0.467(2)	0.025284*
H2	0.912(3)	0.568(5)	−0.199(10)	0.025264*
H3	0.977(2)	0.644(6)	−0.130(9)	0.025264*
H5	1.005(2)	0.6892(14)	0.347(9)	0.023617*

* refined with U_{iso} set as 1.2U_{eq} of the parent O atom.

A single crystal of běhounekite, $0.23 \times 0.18 \times 0.12$ mm, was examined on an Oxford Diffraction Gemini single-crystal diffractometer, with an Atlas CCD detector, using monochromatic Mo-$K\alpha$ radiation. The unit cell was refined from 6630 reflections using the least-squares algorithm in the *CrysalisPro* software package (Oxford Diffraction, 2010). An ω scan rotational method (frame width 0.75º, 25 sec/frame, total 710 frames, completeness 99.65%) was used to collect the three-dimensional intensity data. From a total of 9945 measured reflections, merging of equivalent reflections gave 990 unique reflections; 912 of the reflections were classified as observed with $I_{obs}>3\sigma(I)$. An analytical correction for absorption was applied,

leading to R_{int} of 0.030. Reduction of the data was performed using the *CrysalisPro* software package (Oxford Diffraction, 2010).

The crystal structure of běhounekite was solved by the charge-flipping method using the program *Superflip* (Palatinus and Chapuis, 2007). The structure solution obtained from *Superflip* confirmed the chosen space group, *Pnma*. The data were used for the subsequent refinement based on F^2 using *JANA2006* software (Petříček *et al.*, 2006). All atoms except H were refined anisotropically. Hydrogen atoms were located using difference Fourier maps and refined independently by restraining O−H distances to 0.90(4) Å. The isotropic atomic displacement parameters of hydrogen atoms were evaluated as

TABLE 6. Anistoropic displacement parameters (Å^2) for the crystal structure of běhounekite.

Atom	U_{11}	U_{22}	U_{33}	U_{12}	U_{13}	U_{23}
U1	0.0101(2)	0.0075(2)	0.0111(2)	0	−0.00037(9)	0
S1	0.0080(6)	0.0070(7)	0.0132(7)	−0.0003(6)	−0.0008(5)	0.0001(5)
O1	0.014(3)	0.011(3)	0.034(3)	0	−0.015(3)	0
O2	0.012(2)	0.018(3)	0.033(3)	−0.003(2)	0.0059(16)	−0.0129(19)
O3	0.025(3)	0.010(3)	0.021(3)	0.0019(17)	−0.0011(14)	−0.0002(18)
O4	0.022(2)	0.010(2)	0.019(2)	0.0022(18)	−0.0094(16)	−0.0010(17)
O5	0.014(2)	0.020(3)	0.019(2)	−0.010(2)	0.0059(16)	0.0035(19)
O6	0.0140(19)	0.021(2)	0.023(2)	−0.0026(19)	0.0090(17)	−0.0112(19)
O7	0.022(4)	0.015(4)	0.026(4)	0	0.018(3)	0

The anisotropic displacement factor exponent takes the form:$-2\pi^2[h^2a^{*2}U_{11} + ... + 2hka^*b^*U_{12}]$.

TABLE 7. Bond valence analysis for the crystal structure of běhounekite.

	U1	S1	ΣBV^n	H1	H2	H3	H5	ΣBV^a
O1	0.47		0.47				0.71 × 2→	1.89
O2	0.48 × 2↓		0.48	0.69	0.74			1.91
O3	0.57 × 2↓	1.46	2.03					2.03
O4		1.60	1.60	0.26		0.27		2.13
O5	0.58 × 2↓	1.44	2.02					2.02
O6		1.55	1.55	0.21		0.24		2.00
O7	0.52		0.52	0.72 × 2→				1.96
	4.25	6.05		0.93	0.95	0.98	0.98	

Values are expressed in valence units (v.u.);
BV$^{n/a}$ bond valence sums neglecting/assuming hydrogen-bond contributions;
multiplicity is indicated by × →/ × ↓.

TABLE 8. Selected interatomic distances (in Å) and geometrical parameters for the crystal structure of běhounekite.

U1−O1	2.390(6)
U1−O2	2.385(5)
U1−O2^i	2.385(5)
U1−O3	2.321(5)
U1−O3^i	2.321(5)
U1−O5^{ii}	2.314(4)
U1−O5^{iii}	2.314(4)
U1−O7	2.353(7)
<U1−O>	2.348
V_i (Å^3)	22.48
Δ	0.01296
ECoN	7.946
S1−O3	1.484(6)
S1−O4	1.451(4)
S1−O5	1.488(5)
S1−O6	1.463(4)
<S1−O>	1.471
Δ	0.001
σ^2	2.81
ECoN	3.98

Hydrogen-bond geometry

$D−H⋯A$	D−H	H⋯A	$D⋯A$	$D−H⋯A$
O7−H1⋯O6^{ix}	0.88(3)	2.02(5)	2.731(7)	137(5)
O2−H2⋯O4^{vii}	0.92(6)	1.84(6)	2.748(7)	168(4)
O2−H3⋯O6^{viii}	0.85(5)	1.92(5)	2.681(6)	148(6)
O1−H5⋯O4^v	0.89(3)	1.81(3)	2.688(6)	166(3)

Symmetry codes: (i) x, $−y+\frac{3}{2}$, z; (ii) $−x+\frac{3}{2}$, $−y+1$, $z−\frac{1}{2}$; (iii) $−x+\frac{3}{2}$ $y+\frac{1}{2}$, $z−\frac{1}{2}$; (iv) x, y, $z+1$; (v) $−x+2$, $−y+1$, $−z+1$; (vi) $−x+2$, $y+\frac{1}{2}$, $−z+1$; (vii) x, y, $z−1$; (viii) $−x+2$, $−y+1$, $−z$; (ix) $−x+\frac{3}{2}$, $−y+1$, $z+\frac{1}{2}$; (x) $−x+2$, $y−\frac{1}{2}$, $−z+1$; (xi) x, $−y+\frac{1}{2}$, z; (xii) $−x+\frac{3}{2}$, $y−\frac{1}{2}$, $z−\frac{1}{2}$; (xiii) $−x+\frac{3}{2}$, $y+\frac{1}{2}$, $z+\frac{1}{2}$.
Δ, bond-length distortion after Brown and Shannon (1973);
σ^2, bond-angle distortion (variance) after Robinson et al. (1971);
ECoN, an effective coordination number after Hoppe (1979).

$1.2U_{eq}$ of the parent atom. Details concerning data collection, crystallographic data and the refinement are provided in Table 4. Atom positions and displacement parameters are listed in Tables 5 and 6. For the crystal graphics, *Diamond* software version 3.0 (Brandenburg and Putz, 2005) was employed. Polyhedral geometrical parameters were obtained using *Vesta* software (Momma and Izumi 2008). Bond-valence analysis was carried out according to Brown (2002), using the data of Brown and Altermatt (1985) for ($S^{6+}-O$), Bresse and O'Keefe (1991) for ($U^{4+}-O$) and Brown (2002) for (H−O).

Description of the crystal structure

The crystal structure of běhounekite confirmed the results obtained for the synthetic compound $U^{4+}(SO_4)_2(H_2O)_4$ by Kierkegaard (1956), although his results did not include the positions of the hydrogen atoms. Therefore, natural běhounekite and the synthetic compound of Kierkegaard (1956) are structurally identical. Other synthetic compounds related to $U^{4+}(SO_4)_2(H_2O)_4$ (*Pnma*) have been reported: these contain Ce^{4+} (*Fddd* and *Pnma*) (Casari and Langer, 2007); Zr^{4+} (*Fddd*) (Singer and Cromer, 1959); Np^{4+} (*Pnma*) (Charusnikova *et al.*, 2000); or Pu^{4+} (*Fddd* and *Pnma*) (Jayadevan *et al.*, 1982; Sing Mudher *et al.*, 1988) instead of U^{4+}.

There is one U atom, one S atom, seven O atoms and four H atoms in the asymmetric unit in the běhounekite unit cell. The structure is layered and consists of polyhedra containing uranium and bridging sulphate tetrahedra. Uranium is coordinated by eight oxygen atoms which define a square Archimedean antiprism (Table 7; Fig. 9). The eight ligands include four oxygen atoms belonging to the sulphate groups and four oxygen atoms belonging to H_2O molecules. Each uranium coordination polyhedron is connected via sulphate tetrahedra to other uranium polyhedra ($4\times$) and via hydrogen bonds to the apices of sulphate tetrahedra (Figs 9 and 10). Therefore, the crystal structure is built from sheets of $U(SO_4)_2(H_2O)_4$, perpendicular to [100]. Linkage of the sheets is via hydrogen bonding ($O2-H3\cdots O6$; $O1-H5\cdots O4$) with additional hydrogen bonding within each sheet ($O2-H2\cdots O4$, $O7-H1\cdots O6$). Calculated bond-valence sums (Table 8) confirm that uranium is tetravalent. The sums for the remaining atoms are consistent with their
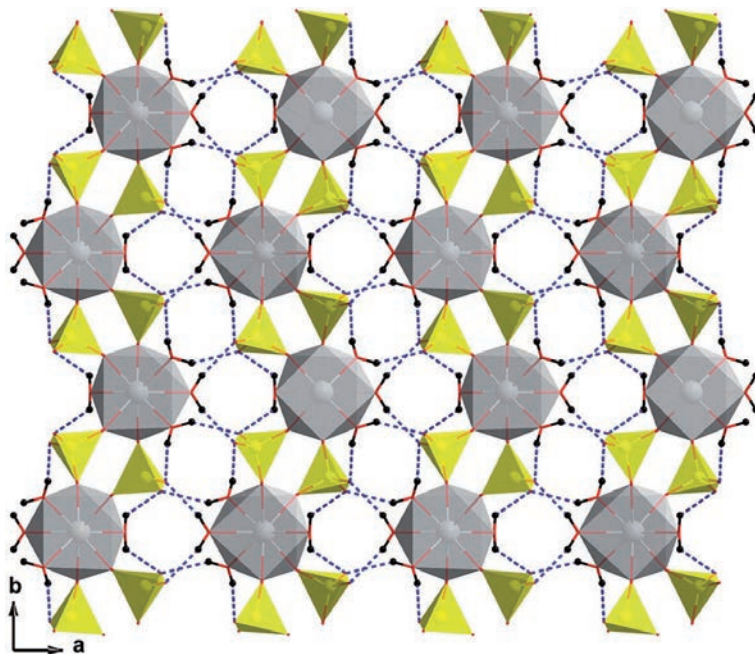

FIG. 9. The crystal structure of běhounekite in projection along [001]. Uranium coordination polyhedra (grey) square Archimedean antiprisms, are linked by sulphate tetrahedra (yellow) and further by hydrogen bonds between sulphate oxygen and hydrogen atoms of H_2O molecules coordinated to uranium.
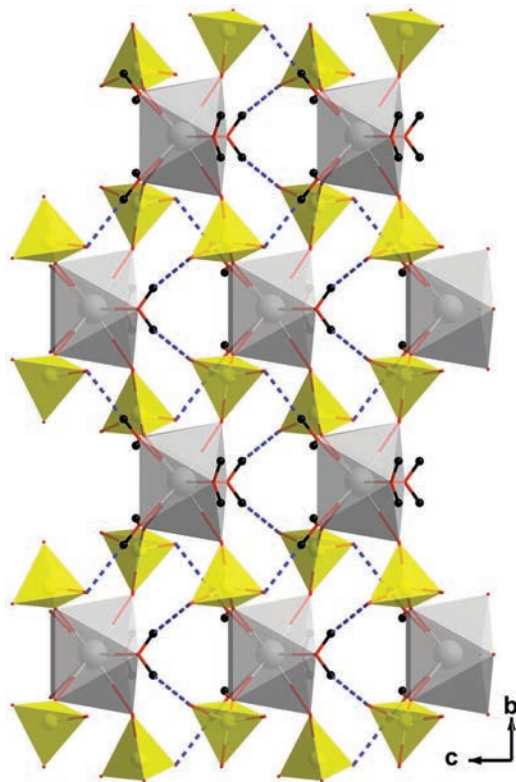
FIG. 10. Connectivity between UO$_8$ polyhedra (grey) and sulphate tetrahedra (yellow) viewed along [100]. Each UO$_8$ square Archimedean antiprism (grey) shares one sulphate tetrahedron and a UO$_8$ polyhedron.

assumed valence states. Interatomic distances, including those for the hydrogen bonds, are listed in Table 8.

Among the structurally related compounds, those containing Ce^{4+} and Pu^{4+} form orthorhombic dimorphs crystallizing in space group *Fddd* (Singer and Cromer, 1959; Jayadevan *et al.*, 1982; Sing Mudher *et al.*, 1988; Casari and Langer, 2007). These two orthorhombic compounds are geometrical isomers; the structural differences lie in the arrangement of sulphate tetrahedra and H$_2$O linked to the UO$_8$ Archimedean antiprism. In modifications with space group *Fddd*, the sulphate tetrahedra lie *trans* to each other in both the tetragonal faces of UO$_8$, whereas in modifications with space group *Pnma*, the sulphate tetrahedra lie *trans* to each other in one tetragonal face and *cis* in the other (Casari and Langer, 2007). The β-Pu(SO$_4$)$_2$(H$_2$O)$_4$

polymorph can be obtained by heating α-Pu(SO$_4$)$_2$(H$_2$O)$_4$ very slowly to 120ºC (Jayadevan *et al.*, 1982). This α−β transition can also be achieved by hydrothermal equilibration (Jayadevan *et al.*, 1982) similar to the α−β transformation of Ce(SO$_4$)$_2$(H$_2$O)$_4$ (Casari and Langer, 2007). In case of běhounekite, or synthetic U(SO$_4$)$_2$(H$_2$O)$_4$, no geometrical isomerism has been observed. However, the possible existence of such a phase is open to question.

Acknowledgements

References

Brandenburg, K. and Putz, H. (2005) *DIAMOND Version 3*. Crystal Impact GbR, Postfach 1251, D-53002 Bonn, Germany.

Bresse, N.E. and O'Keeffe, M. (1991) Bond-valence parameters for solids. *Acta Crystallographica*, **B47**, 192−197.

Brown, I.D. (2002) *The Chemical Bond in Inorganic Chemistry. The Bond Valence Model*. Oxford University Press, Oxford, UK.

Brown, I.D. and Altermatt, D. (1985) Bond-valence parameters obtained from a systematic analysis of the inorganic crystal structure database. *Acta Crystallographica*, **B41**, 244−248.

Brown, I.D. and Shannon, R.D. (1973) Empirical bond-strength bond-length curves for oxides. *Acta Crystallographica*, **A29**, 266−282.

Burns, P.C., Finch, R.J., Hawthorne, F.C., Miller, M.L. and Ewing, R.C. (1997) The crystal structure of ianthinite, $[U^{4+}(UO_2)_4O_6(OH)_4(H_2O)_4](H_2O)_5$: a possible phase for Pu^{4+} incorporation during the oxidation of spent nuclear fuel. *Journal of Nuclear Materials*, **249**, 199−206.

Casari, B.M. and Langer, V. (2007) Two $Ce(SO_4)_2 \cdot 4H_2O$ polymorphs: crystal structure and thermal behavior. *Journal of Solid State Chemistry*, **180**, 1616−1622.

Čejka, J. (1999) Infrared spectroscopy and thermal analysis of the uranyl minerals. Pp. 521−622 in: *Uranium: mineralogy, geochemistry and the environment* (P.C. Burns and R. Finch, editors). Reviews in Mineralogy, **38**. Mineralogical Society of America, Washington DC.

Čejka, J. (2007) Vibrational spectroscopy of uranyl minerals − infrared and Raman spectroscopy of the uranyl minerals III. Uranyl sulphates. *Bulletin mineralogicko-petrologického oddělení Národního muzea (Praha)*, **14−15**, 40−46, [in Czech].

Čejka, J. and Urbanec, Z. (1990) Secondary uranium minerals. *Transactions of the Czechoslovak Academy of Sciences, Mathematical and Natural History Series*, **100**, 1−93.

Charusnikova, I.A., Krot, N.N. and Starikova, Z.A. (2000) Crystal structure and spectral characteristics of double sodium neptunium(IV) sulfate. *Radiochemistry*, **42**, 434−438.

Chernyaev, I.I. (editor) (1964) *Complex compounds of uranium*. Nauka, Moscow, 492 pp., [in Russian].

Delobel, R. (1970) *Etude structurale des hydrates des sulfates d'uranyle et d'uranium IV*. Thesis, University of Lille, 67 pp.

Finch, R. and Murakami, T. (1999) Systematics and paragenesis of uranium minerals. Pp. 91−179 in: *Uranium: mineralogy, geochemistry and the environment* (P.C. Burns and R. Finch, editors). Reviews in Mineralogy, **38**. Mineralogical Society of America, Washington DC.

Hawthorne, F.C. and Schindler, M. (2008) Understanding the weakly bonded constituents in oxysalt minerals. *Zeitschrift für Kristallographie*, **223**, 41−68.

Hoppe, R. (1979) Effective coordination numbers (ECoN) and mean fictive ionic radii (MEFIR). *Zeitschrift für Kristallographie*, **150**, 23−52.

Jayadevan, N.C., Singh Mudher, K.D. and Chackraburtty, D.M. (1982) The crystal structures of α-and β-forms of plutonium(IV) sulphate tetrahydrate. *Zeitschrift für Kristallographie*, **161**, 7−13.

Kierkegaard, P. (1956) The crystal structure of $U(SO_4)_2(H_2O)_4$. *Acta Chemica Scandinavica*, **10**, 599−616.

Langmuir, D. (1978) Uranium solution-mineral equilibria at low temperatures with applications to sedimentary ore. *Geochimica et Cosmochimica Acta*, **42**, 547−569.

Leroy, J.-M. (1966) *Contribution à la connaissance physique et chimique des composés oxygénés de l'uranium aux degrés d 'oxydation 4, 5 et 6*. PhD Thesis, University of Lille, 115 pp.

Leroy, J.-M. (1967) Contribution à la connaissance physique et chimique des composés oxygénés de l'uranium aux degrés d'oxydation 4, 5 et 6. *Revue de Chimie Minérale*, **4**, 129−180.

Libowitzky, E. (1999) Correlation of O−H stretching frequencies and O−H⋯O hydrogen bond lengths in minerals. *Monatshefte für Chemie*, **130**, 1047−1059.

Malinka, V.I., Nikanovich, M.V. and Umreiko, D.S. (1979) Calculation and investigation of the vibrational spectrum of the diuraniumsulfate fragment in aquasulfate complexes of tetravalent uranium. *Doklady Akademii Nauk BSSR*, **23**, 808−811, [in Russian].

Malinka, V.I., Nikanovich, M.V. and Umreiko, D.S. (1981) Calculation and investigation of the vibrational spectrum of the tetraaquadisulfate of tetravalent uranium. *Journal of Applied Spectroscopy*, **34**, 173−177.

Momma K. and Izumi, F. (2008) VESTA: a three-dimensional visualization system for electronic and structural analysis. *Journal of Applied Crystallography*, **41**, 653−658.

Ondruš, P., Veselovský, F., Hloušek, J., Skála, R., Vavřín, I., Frýda, J., Čejka, J. and Gabašová, A. (1997*a*) Secondary minerals of the Jáchymov (Joachimsthal) ore district. *Journal of the Czech Geological Society*, **42**, 3−76.

Ondruš, P., Veselovský, F., Skála, R., Císařová, I., Hloušek, J., Frýda, J., Vavřín, I., Čejka, J. and Gabašová, A. (1997*b*) New naturally occurring phases of secondary origin from Jáchymov (Joachimsthal). *Journal of the Czech Geological Society*, **42**, 77−107.

Ondruš, P., Veselovský, F., Gabašová, A., Hloušek, J., Šrein, V., Vavřín, I., Skála R., Sejkora, J. and Drábek, M. (2003) Primary minerals of the Jáchymov ore district. *Journal of the Czech Geological Society*, **48**, 19−147.

Oxford Diffraction (2010) *CrysAlis CCD and CrysAlis RED*. Oxford Diffraction Ltd, Yarnton, UK.

Palatinus, L. and Chapuis, G. (2007) *Superflip* − a computer program for the solution of crystal structures by charge flipping in arbitrary dimensions. *Journal of Applied Crystallography*, **40**, 451−456.

Petříček, V., Dušek, M. and Palatinus, L. (2006) *Jana2006. The crystallographic computing system*. Institute of Physics, Prague, Czech Republic.

Plášil, J., Fejfarová, K., Novák, M., Dušek, M., Sejkora, J., Škoda, R., Hloušek, J. and Majzlan, J. (2011) Běhounekite, IMA 2010-046. CNMNC Newsletter No. 7, February 2011, page 28; *Mineralogical Magazine*, **75**, 27−31.

Pouchou, J.L. and Pichoir, F. (1985) "PAP" (φρZ) procedure for improved quantitative microanalysis. Pp. 104−106 in: *Microbeam Analysis* (J.T. Armstrong, editor). San Francisco Press, San Francisco, California, USA.

Robinson, K., Gibbs, G.V. and Ribbe, P.H. (1971) Quadratic elongation: a quantitative measure of distortion in coordination polyhedra. *Science*, **172**, 567−570.

Schindler, M. and Hawthorne, F.C. (2008) The stereochemistry and chemical composition of interstitial complexes in uranyl-oxysalt minerals. *The Canadian Mineralogist*, **46**, 467−501.

Sing Mudher, K.D., Krishnan, K., Chackraburtty, D.M. and Jayadevan, N.C. (1988) Structural and thermal investigations of tetrasulphates of uranium(IV) and plutonium(IV). *Journal of the Less Common Metals*, **143**, 173−182.

Singer, J. and Cromer, D.T. (1959) The crystal structure analysis of zirconium sulphate tetrahydrate. *Acta Crystallographica*, **12**, 719−723.

Smith, D.G.W. and Nickel, E.H. (2007) A system for codification for unnamed minerals: report of the Subcommittee for Unnamed Minerals of the IMA Commission on New Minerals, Nomenclature and Classification. *The Canadian Mineralogist*, **45**, 983−1055.

Taylor, S.R. and McLennan, S.M. (1985) *The Continental Crust: its Composition and Evolution*. Blackwell, Oxford, UK, 328 pp.

Tvrdý, J. and Plášil, J. (2010) Jáchymov − Reiche Erzlagerstätte und Radonbad im böhmischen Westerzgebirge. *Aufschluss*, **61**, 277−292.

Umreiko, D.S. and Nikanovich, M.V. (1984) Vibrational spectroscopy and structural analysis of complex uranium compounds (review). *Journal of Applied Spectroscopy*, **41**, 1303−1314.